Preparation, ^1H NMR Spectrum and Structure of *cis*-Diamminebis(1-methylcytosine)platinum(II) Nitrate–1-Methylcytosine. Cis Steric Effects in Pyrimidine Ring-Bound *cis*-Bis(nucleic acid base)platinum(II) Compounds

John D. Orbell,[1a] Luigi G. Marzilli,*[1b] and Thomas J. Kistenmacher*[1a]

Contribution from the Departments of Chemistry, The Johns Hopkins University, Baltimore, Maryland 21218, and Emory University, Atlanta, Georgia 30322. *Received January 12, 1981. Revised Manuscript Received April 14, 1981*

Abstract: The synthesis, solution ^1H NMR spectrum, and solid-state molecular and crystal structure of *cis*-diamminebis(1-methylcytosine)platinum(II) nitrate–1-methylcytosine, $[(NH_3)_2Pt(1\text{-}MeC)_2](NO_3)_2\cdot 1\text{-}MeC$, are reported. Single crystals of the coordination compound were identified as belonging to the triclinic system, space group $P\bar{1}$, with the following primary crystallographic data: $a = 13.624$ (5) Å, $b = 13.978$ (4) Å, $c = 7.012$ (2) Å, $\alpha = 95.42$ (2)°, $\beta = 99.01$ (3)°, $\gamma = 110.17$ (2)°, $V = 1221.4$ Å^3, $Z = 2$ [based on a molecular weight of 728.4 for $Pt(NH_3)_2(C_5N_3OH_7)_2(NO_3)_2\cdot(C_5N_3OH_7)$], $D_{measd} = 1.980$ (3) g/cm^3, $D_{calcd} = 1.973$ g/cm^3. A structural model was readily developed by conventional Patterson and Fourier methods and has been refined by full-matrix least-squares techniques on the basis of 6829 nonzero structure-factor amplitudes to an R value of 0.059. The *cis*-$[(NH_3)_2Pt(1\text{-}MeC)_2]^{2+}$ cation is nearly square planar with the two independent 1-MeC ligands showing N(3)–Pt bonding and arranged in a head-to-tail fashion such that the complex cation possesses approximate $2(C_2)$ molecular symmetry. Weak intracomplex, interbase hydrogen bonds of the type $N(4)H_2\cdots O(2)$ are observed. Principal intracomplex geometrical parameters are as follows: Pt–N(ammine) = 2.033 (7) Å, 2.031 (7) Å; Pt–N(3)(1-MeC) = 2.031 (6) Å, 2.040 (6) Å; N(ammine)–Pt–N(ammine) angle = 89.0 (3)°; N(3)(1-MeC)–Pt–N(3)(1-MeC) angle = 92.6 (2)°; interbase dihedral angle = 102.3°; base/PtN_4 coordination plane dihedral angles = 101.2° and 102.4°. The geometries of the coordinated 1-MeC bases are very similar to that displayed by the 1-MeC base of crystallization. The 1-MeC of crystallization forms an intimate stacking interaction with one of the two cis-coordinated 1-MeC ligands of the complex cation. Base/base and base/nitrate anion stacking and interbase and base···nitrate anion hydrogen bonding are predominant modes of interaction in the solid. The ^1H NMR spectrum of the coordination compound in Me_2SO-d_6 shows resonances for coordinated and uncoordinated 1-MeC bases. The resonance for the exocyclic amino group, $N(4)H_2$, of the uncoordinated 1-MeC base is a broad singlet, while the amino resonances for the coordinated 1-MeC ligands are two well-resolved singlets. The resolution of the $N(4)H_2$ resonances for the coordinated 1-MeC bases implies restricted rotation about the C(4)–N(4) bond. Finally, a detailed comparison is made among the conformational aspects of the present compound and those displayed by other *cis*-bis(pyrimidine ring-bound)platinum(II) complexes.

Introduction

Although it has been over a decade now since Rosenberg and co-workers[2] described the clinical success of platinum(II) antitumor agents (notably, *cis*-$[(NH_3)_2PtCl_2]$), the mechanism of action of such agents remains in detail unknown. There have been much data presented implicating DNA as the primary target for the Pt(II) drugs,[3,4] with increasing evidence that regions rich in guanosine (Guo) and cytidine (Cyd) residues show preferential binding of Pt(II) reagents.[5-8] As the apparent formation constants for the $[(NH_3)_2Pt(\text{nucleoside})(H_2O)]^{2+}$ complexes of adenosine (Ado), Guo, and Cyd [log K = 3.6, 3.7, and 3.5, respectively][9] do not suggest a thermodynamic basis for the preferential binding to Guo-Cyd rich regions, it has been concluded that kinetic effects predominate. In this regard, it was indicated early[10] that reaction rates were higher for Guo than for Ado or Cyd. In addition, Tobias and co-workers[11] reported that the order of nucleophilicity toward *cis*-$[(NH_3)_2Pt(H_2O)_2]^{2+}$ and *cis*-$[(NH_3)_2PtCl_2]$ for the 5′-nucleoside monophosphates was GMP > AMP ≫ CMP. Consistent with this trend, Inagaki and Kidani[12] recently reported that the major product of the reaction between *cis*-$[(NH_3)_2PtCl_2]$ and the dinucleoside monophosphate GpC(C3′p5′G) was the complex *cis*-$[(NH_3)_2Pt(GpC)_2]$, with the two dinucleoside monophosphate ligands bound through N(7) of the Guo residues. However, Jordanov and Williams[13] found in a study of the reaction of $[(en)PtCl_2]$ with CpG(G3′p5′C) that complexation took place first at the Cyd residue. Similarly, Chottard and co-workers[14] found that reaction of *cis*-$[(NH_3)_2Pt(H_2O)_2](NO_3)_2$ with the dinucleoside monophosphates GpC and ApC appeared to indicate a greater affinity for Cyd than for Guo or Ado.

In the work of Jordanov and Williams[13] and, particularly, that of Chottard,[14] spectroscopic evidence was invoked for the formation of 1:1 Pt(II)/dinucleoside monophosphate complexes, $[(en)Pt(CpG)]$[13] and $[(NH_3)_2Pt(GpC)]$,[14] in which both N(3) of Cyd and N(7) of Guo were bound to the same Pt(II) center and some degree of intramolecular base/base stacking was present. Such Pt(II)/dinucleoside monophosphate complexes could be considered as models for one of the leading speculations as to the mode of

(1) (a) Johns Hopkins University. (b) Emory University.
(2) Rosenberg, B.; Van Camp, L.; Trosko, J. E.; Mansour, V. H. *Nature (London)* **1969**, *222*, 385. For a recent review, see: *Biochimie* **1978**, *60*, No. 9.
(3) Roberts, J. J.; Thomson, A. J. *Prog. Nucleic Acid Res. Mol. Biol.* **1979**, *22*, 71.
(4) Roberts, J. J. *Adv. Inorg. Biochem.*, in press.
(5) de Castro, B.; Kistenmacher, T. J.; Marzilli, L. G. in "Trace Elements in the Pathogenesis and Treatment of Inflammatory Conditions"; Rainsford, K. D., Brune, K., Whitehouse, M. W., Eds.; Agents and Actions: Basel, 1981.
(6) (a) Marzilli, L. G.; Kistenmacher, T. J.; Eichhorn, G. L. In "Nucleic Acid-Metal Ion Interactions"; Spiro, T. G., Ed.; Wiley: New York, 1980; Chapter 5. (b) Barton, J. K.; Lippard, S. J. *Ibid.*; Chapter 2. (c) Marzilli, L. G. *Adv. Inorg. Biochem.*, in press.
(7) Stone, P. J.; Kelman, A. J.; Sinex, F. M. *Nature (London)* **1974**, *251*, 736.
(8) Cohen, G. L.; Ledner, J. A.; Bauer, W. R.; Ushay, H. M.; Caravana, C.; Lippard, S. J. *J. Am. Chem. Soc.* **1980**, *102*, 2487.
(9) Scovell, W. M.; O'Connor, T. *J. Am. Chem. Soc.* **1977**, *99*, 120. For a critical update see: Vestues, P. I.; Martin, R. B. *Ibid.* **1981**, *102*, 806.
(10) Robins, A. B. *Chem.-Biol. Interact.* **1973**, *6*, 35; *7*, 11.
(11) Mansy, S.; Chu, G. Y. H.; Duncan, R. E.; Tobias, R. S. *J. Am. Chem. Soc.* **1978**, *100*, 607.
(12) Inagaki, K.; Kidani, Y. J. *Inorg. Biochem.* **1979**, *11*, 39.
(13) Jordanov, J.; Williams, R. J. P. *Bioinorg. Chem.* **1978**, *8*, 77.
(14) Chottard, J. C.; Girault, J. P.; Chottard, G.; Lallemand, J. Y.; Mansuy, D. *J. Am. Chem. Soc.* **1980**, *102*, 5565.

0002-7863/81/1503-5126$01.25/0

action of Pt(II) antitumor drugs, namely, the critical lesion being an intrastrand cross-linkage.[5-6,8,15,16] In regions of high Guo-Cyd content, one may envision three main types of cross-linking modes involving the endocyclic N(3) atom of cytosine and the endocyclic N(7) and N(1) atoms of the imidazole and pyrimidine rings, respectively, of guanine.[17] These modes may be represented as follows: (1) G[N(7)]-Pt-G[N(7)]; (2) G[N(7)]-Pt-G[N(1)] or G[N(7)]-Pt-C[N(3)]; (3) C[N(3)]-Pt-C[N(3)], C[N(3)]-PtG[N(1)], or G[N(1)]-Pt-G[N(1)]. Each of the above modes, for the present, can be considered kinetically accessible, although different potential interactions between the cis-coordinated bases are expected depending upon the number and nature of the exocyclic substituents contiguous to the Pt atom binding sites.

Several model complexes for the type 1 cross-link mode containing Pt(II) and Guo,[18,19] 5′-IMP (inosine 5′-monophosphate),[20-23] 5′-GMP,[24] and the phosphate methyl ester of 5′-GMP [Me-5′-GMP][25] have been characterized in detail by X-ray crystallographic methods. In addition, the structure of a type 2 model complex *cis*-$[(NH_3)_2Pt$(1-methylcytosine)(9-ethylguanine)$]^{2+}$ has recently been reported by Faggiani, Lock, and Lippert.[26] Finally, Wu and Bau[27] have described the structure of the *cis*-$[(NH_3)_2Pt(3'\text{-CMP})_2]^{2-}$ anion, a model for a type 3 cross-link mode. Unfortunately, the crystal chemistry of this latter complex is complicated and the reported analysis[27] does not allow a definitive assessment of many of the most intriguing geometrical aspects of the molecular anion.

We have recently been particularly interested in the binding of Pt(II) to the endocyclic N-atom binding sites of the pyrimidine rings of the nucleic acid bases.[17,28,29] In the context of the previous discussion, we felt it particularly important to characterize in detail a *cis*-bis(N(3)-bound)platinum(II) complex of Cyd or one of its derivatives. One of our primary goals was the elucidation of the intramolecular interactions between the two cis-coordinated and ortho-disubstituted bases. Utilization of the modified base 1-methylcytosine (1-MeC) (Figure 1) has allowed the preparation of the compound *cis*-$[(NH_3)_2Pt(1\text{-MeC})_2](NO_3)_2\cdot$(1-MeC), which we have characterized extensively by ^1H NMR and X-ray diffractions methods. We have found it necessary to propose a stereochemical convention in order to compare the primary conformational features of the above complex (e.g., the interbase dihedral angle, base/PtN_4 coordination plane dihedral angles) to those in related systems.

Experimental Section

(a) Reagents. K_2PtCl_4 was supplied by Matthey Bishop; Me_2SO-d_6 was supplied by Aldrich. Common chemicals were obtained from other scientific supply houses. The 1-MeC free base was synthesized in our laboratories by an extensive modification[30] of the procedure of Sakai, Pogolotti, and Santi.[31]

(b) *cis*-$[Pt(NH_3)_2(1\text{-MeC})_2](NO_3)\cdot$1-MeC. An aqueous solution of 0.27 g (1.6 mmol) of $AgNO_3$ was added to a suspension of 0.39 g (0.8 mmol) of *cis*-$[Pt(NH_3)_2I_2]$[32] in 10 mL of distilled water (total volume ~20 mL). The suspension was gently heated at ~60 °C (with stirring) for 30 min, and the insoluble AgI was filtered over Celite. The pale yellow filtrate was heated to ~65 °C, and an aqueous solution containing 0.26 g (2.1 mmol) of 1-MeC, also heated to ~65 °C, was added to it with stirring. The pH of the final solution was ~5. The mole ratio of 1-MeC to Pt in this preparation was 2.63 (a 31% excess of 1-MeC relative to a 2:1 base/Pt stoichiometry). After several days of slow evaporation of the solvent, clusters of well-formed, colorless platelets were harvested. A density measurement and preliminary X-ray data were consistent with the formulation $Pt(NH_3)_2(1\text{-MeC})_2(NO_3)_2\cdot$1-MeC. This was later confirmed by the full X-ray analysis.

A subsequent preparation at 2:1 1-MeC/Pt stoichiometry produced crystals identical with those described above (as shown by their density and X-ray diffraction spectra). However, in this case the harvested crystals were smaller and of a relatively inferior quality. Also, the presence of one or more "platinum purple" byproducts[33] made a clean batch of crystals difficult to obtain.

(c) ^1H NMR Data. ^1H NMR spectra were recorded on a Varian CFT-20 spectrometer in the proton mode by using standard Fourier transform techniques. Me_2SO-d_6 was used as the solvent and the concentration of the samples (utilizing crystalline material) was approximately 0.15 M. With use of a spectral width of 1205 Hz and a pulse of 18 μs, the acquisition time for 120 transients was 34 s (8192 data points).

(d) Collection and Reduction of the X-ray Intensity Data. The external morphology of the transparent crystals of the title compound was that of elongated platelets. Oscillation and Weissenberg photography showed the crystal class to be triclinic and allowed the computation of preliminary unit-cell data. A single, well-formed crystal was selected and cleaved perpendicular to its long axis (*b*) to give a platelet with the following faces and dimensions: (100)-($\bar{1}$00), 0.06 mm; (001)-(00$\bar{1}$), 0.22 mm; (010)-(0$\bar{1}$0), 0.24 mm. This platelet was mounted on a thin glass fiber and positioned on a Syntex P$\bar{1}$ automated diffractometer. Precise values for the unit-cell dimensions, together with their standard deviations, were derived from a least-squares fit to the setting angles for 15 carefully selected and centered reflections. The crystallographic *b* axis was approximately aligned along the ϕ axis of the spectrometer. The crystal density was measured by the neutral buoyancy method in a mixture of carbon tetrachloride and bromoform and indicated two formula units of the title compound per cell. Relevant crystallographic data are collected in Table I.

Table I. Crystal Data for *cis*-$[(NH_3)_2Pt(1\text{-MeC})_2](NO_3)_2\cdot$1-MeC

$a = 13.624$ (5) Å	$V = 1221.4$ Å^3
$b = 13.978$ (4) Å	$[Pt(NH_3)_2(C_5N_3OH_7)_2]^{2+}(NO_3^-)_2\cdot(C_5N_3OH_7)$
$c = 7.012$ (2) Å	space group P$\bar{1}$
$\alpha = 95.42$ (2)°	mol wt 728.4
$\beta = 99.01$ (3)°	$D_{measd} = 1.980$ (3) g/cm^3
$\gamma = 110.17$ (2)°	D_{calcd} ($Z = 2$) = 1.973 g/cm^3

With use of graphite-monochromatized Mo Kα radiation ($\bar{\lambda}$ = 0.71069 Å), the intensities of 7694 reflections (including standards) in the $+h$ hemisphere (to $2\theta = 60°$) were surveyed. The θ-2θ scan mode was employed with a constant scan rate (2θ) of 2° min^{-1}. The intensities of three standards were monitored every 100 reflections and showed no systematic variation over the course of the experiment. The 6829 reflections with net intensities above zero (out of a unique set of 7163) were assigned observational variances on the basis of the following equation: $\sigma^2(I) = S + (B_1 + B_2)(T_S/2T_B)^2 + (pI)^2$, where S, B_1, and B_2 are the scan and extreme background counts, T_S and T_B are the scan and individual background counting times ($T_B = T_S/2$ for all data points), and p, which represents an esimate of the error proportional to the diffraction intensity,[34] was given a value of 0.03. Reflections with net negative intensity were assigned F's and weights equal to zero.

The intensities and their standard deviations were corrected for Lorentz and polarization effects and for the effect of absorption (maximum and minimum transmission factors of 0.68 and 0.28, respectively, on the basis of the above face assignments and crystal dimensions and a calculated linear absorption coefficient of 61.2 cm^{-1}). An approximate scale factor was derived by the method of Wilson.[35]

(15) Marzilli, L. G. *Prog. Inorg. Chem.* **1977**, *23*, 255.
(16) Kelman, A. D.; Buchbinder, M. *Biochimie* **1978**, *60*, 893.
(17) Kistenmacher, T. J.; de Castro, B.; Wilkowski, K.; Marzilli, L. G. *J. Inorg. Biochem.*, in press.
(18) Gellert, R. W.; Bau, R. *J. Am. Chem. Soc.* **1975**, *97*, 7379.
(19) Cramer, R. E.; Dahlstrom, P. L. *J. Clin. Hematol. Oncol.* **1977**, *7*, 330. Cramer, R. E.; Dahlstrom, P. L.; Seu, M. J. T.; Norton, T.; Kashiwagi, M. *Inorg. Chem.* **1980**, *19*, 148.
(20) Goodgame, D. M. L.; Jeeves, I.; Phillips, F. L.; Skapski, A. C. *Biochim. Biophys. Acta* **1975**, *378*, 153.
(21) Bau, R.; Gellert, R. W.; Lehovec, S. M.; Louie, S. *J. Clin. Hematol. Oncol.* **1977**, *7*, 51.
(22) Kistenmacher, T. J.; Chiang, C. C.; Chalilpoyil, P.; Marzilli, L. G. *Biochem. Biophys. Res. Commun.* **1978**, *84*, 70.
(23) Kistenmacher, T. J.; Chiang, C. C.; Chalilpoyil, P.; Marzilli, L. G. *J. Am. Chem. Soc.* **1979**, *101*, 1143.
(24) Bau, R.; Gellert, R. W. *Biochimie* **1978**, *60*, 1040.
(25) Marzilli, L. G.; Chalilpoyil, P.; Chiang, C. C.; Kistenmacher, T. J. *J. Am. Chem. Soc.* **1980**, *102*, 2480.
(26) Faggiani, R.; Lock, C. J. L.; Lippert, B. *J. Am. Chem. Soc.* **1980**, *102*, 5419.
(27) Wu, S. M.; Bau, R. *Biochem. Biophys. Res. Commun.* **1979**, *88*, 1435.
(28) Kistenmacher, T. J.; Wilkowski, K.; de Castro, B.; Chiang, C. C.; Marzilli, L. G. *Biochem. Biophys. Res. Commun.* **1979**, *91*, 1521.
(29) de Castro, B.; Chiang, C. C.; Wilkowski, K.; Marzilli, L. G.; Kistenmacher, T. *J. Inorg. Chem.* **1981**, *20*, 1835.
(30) Kistenmacher, T. J.; Rossi, M.; Caradonna, J. P.; Marzilli, L. G. *Adv. Mol. Relaxation Interact. Processes* **1979**, *15*, 119.
(31) Sakai, T. T.; Pogolotti, A. L.; Santi, D. V. *J. Heterocyl. Chem.* **1968**, *5*, 849.
(32) Dhara, S. C. *Indian J. Chem.* **1970**, *8*, 193.
(33) Barton, J. K.; Szalda, D. J.; Rabinowitz, H. N.; Waszczak, J. V.; Lippard, S. J. *J. Am. Chem. Soc.* **1979**, *101*, 1434 and references therein.
(34) Busing, W. R.; Levy, H. A. *J. Chem. Phys.* **1957**, *26*, 563.

Table II. Final Nonhydrogen Atom Coordinates for *cis*-$[(NH_3)_2Pt(1\text{-}MeC)_2](NO_3)_2\cdot 1\text{-}MeC$[a]

atom	x	y	z	atom	x	y	z
Pt[b]	15706 (2)	22388 (2)	26946 (4)	C(5B)	3634 (6)	4861 (6)	673 (10)
N(10)	380 (5)	903 (5)	2848 (10)	C(6B)	4066 (6)	5544 (6)	2334 (11)
N(11)	552 (6)	2996 (5)	2928 (10)	O(2C)	1558 (6)	5494 (5)	4538 (8)
O(2A)	1661 (5)	880 (4)	−836 (7)	N(1C)	2115 (6)	6775 (5)	2740 (9)
N(1A)	2916 (5)	237 (5)	241 (9)	N(3C)	1253 (5)	5019 (5)	1256 (9)
N(3A)	2522 (5)	1419 (4)	2339 (8)	N(4C)	986 (6)	4602 (5)	−2058 (9)
N(4A)	3425 (6)	1934 (5)	5533 (9)	C(1C)	2531 (9)	7572 (7)	4510 (13)
C(1A)	2720 (9)	−372 (7)	−1690 (12)	C(2C)	1621 (6)	5739 (6)	2886 (11)
C(2A)	2326 (6)	850 (5)	511 (9)	C(4C)	1352 (6)	5325 (6)	−478 (10)
C(4A)	3253 (6)	1366 (5)	3822 (10)	C(5C)	1843 (7)	6367 (6)	−672 (11)
C(5A)	3829 (7)	706 (6)	3532 (12)	C(6C)	2220 (7)	7060 (6)	963 (11)
C(6A)	3647 (7)	170 (6)	1742 (12)	N(41)	5226 (6)	2003 (5)	−288 (9)
O(2B)	3106 (5)	4034 (4)	5847 (6)	O(41)	4706 (6)	2554 (5)	−94 (10)
N(1B)	3874 (5)	5275 (4)	4106 (8)	O(42)	5784 (6)	1847 (6)	1118 (9)
N(3B)	2738 (5)	3596 (4)	2529 (7)	O(43)	5187 (7)	1595 (6)	−1963 (10)
N(4B)	2433 (5)	3193 (5)	−824 (8)	N(51)	574 (6)	8426 (5)	2627 (10)
C(1B)	4293 (7)	6026 (6)	5904 (11)	O(51)	0 (7)	7643 (7)	3064 (15)
C(2B)	3226 (6)	4285 (5)	4230 (9)	O(52)	787 (8)	8549 (8)	1059 (12)
C(4B)	2927 (5)	3860 (5)	771 (9)	O(53)	956 (7)	9182 (6)	3973 (12)

[a] Estimated standard deviations in the least significant figure are enclosed in parentheses here and in all the following tables. [b] Parameters × 10^5; for all other atoms, parameters × 10^4.

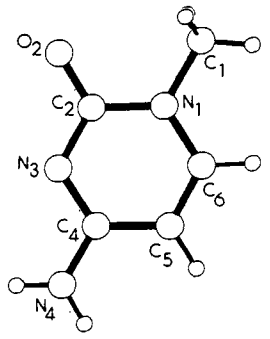

Figure 1. Molecular structure and atomic numbering scheme for the free base 1-methylcytosine (1-MeC).

(e) Solution and Refinement of the Structure. The positional coordinates of the Pt atom were deduced from a three-dimensional Patterson synthesis. A subsequent structure factor-difference Fourier calculation allowed the positioning of the 37 remaining nonhydrogen atoms of the asymmetric unit. Several cycles of isotropic and anisotropic least-squares refinement, minimizing the quantity $\sum w(|F_o| - |F_c|)^2$, where $w = 4F_o^2/\sigma^2(F_o^2)$, gave an R value ($=\sum||F_o| - |F_c||/\sum|F_o|$) of 0.064. At this stage, a difference Fourier synthesis yielded coordinates for all 27 hydrogen atoms; the isotropic temperature factor of each hydrogen atom was fixed at a value approximately 1.0 Å^2 higher than the value for the atom to which it was bonded. The contributions from the hydrogen atoms were included in subsequent cycles of refinement, but no attempt was made to refine either their positional or their thermal parameters. Two further cycles of refinement led to convergence (all shift/error less than 0.7) and to a final R value of 0.059. The final weighted R value $[=(\sum w(|F_o| - |F_c|)^2/\sum w|F_o|^2)^{1/2}]$ and goodness-of-fit value $[=(\sum w|F_o| - |F_c|)^2/(NO - NV))^{1/2}$, where NO = 6829 nonzero observations and NV = 343 variables] were 0.061 and 2.22, respectively. A final difference Fourier map was essentially featureless, with the exception of two peaks at approximate heights of 5 e/A^3 near the Pt atom.

Neutral scattering curves for the nonhydrogen atoms[36] and the hydrogen atoms[37] were taken from common sources. Anomalous dispersion corrections were applied to the scattering curves for all nonhydrogen atoms.[38] Final atomic positions for the nonhydrogen atoms are collected in Table II. Tables of anisotropic thermal parameters, parameters for the hydrogen atoms, and final observed and calculated structure factor amplitudes have been deposited.[39] The crystallographic calculations were performed with a standard set of computer programs.[40]

(35) Wilson, A. J. C. *Nature (London)* **1942**, *150*, 152.
(36) Hanson, H. P.; Herman, F.; Lea, J. D.; Skillman, S. *Acta Crystallogr.* **1964**, *17*, 1040.
(37) Stewart, R. F.; Davidson, E. R.; Simpson, W. T. *J. Chem. Phys.* **1965**, *42*, 3175.
(38) Cromer, D. T.; Liberman, D. *J. Chem. Phys.* **1970**, *53*, 1891.
(39) See paragraph at end of the paper regarding supplementary material.

Table III. Molecular Geometry for *cis*-$[(NH_3)_2Pt(1\text{-}MeC)_2](NO_3)_2\cdot 1MeC$

(a) Primary Coordination Sphere about the Pt Atom

	Bond Lengths, Å		
Pt-N(1)	2.033 (7)	Pt-N(3A)	2.031 (6)
Pt-N(11)	2.031 (7)	Pt-N(3B)	2.040 (6)
	Bond Angles, deg		
N(10)-Pt-N(11)	89.0 (3)	N(11)-Pt-N(3A)	176.7 (3)
N(10)-Pt-N(3A)	88.8 (3)	N(11)-Pt-N(3B)	89.7 (3)
N(10)-Pt-N(3B)	178.6 (3)	N(3A)-Pt-N(3B)	92.6 (2)

(b) 1-Methylcytosine Bases

	A	B	C
	Bond Lengths, Å		
N(1)-C(2)	1.38 (1)	1.38 (1)	1.39 (1)
C(2)-N(3)	1.38 (1)	1.37 (1)	1.35 (1)
N(3)-C(4)	1.35 (1)	1.36 (1)	1.34 (1)
C(4)-C(5)	1.42 (1)	1.42 (1)	1.41 (1)
C(5)-C(6)	1.34 (1)	1.34 (1)	1.33 (1)
N(1)-C(6)	1.37 (1)	1.37 (1)	1.36 (1)
N(1)-C(1)	1.46 (1)	1.46 (1)	1.48 (1)
C(2)-O(2)	1.22 (1)	1.24 (1)	1.25 (1)
C(4)-N(4)	1.32 (1)	1.31 (1)	1.33 (1)
	Bond Angles, deg		
C(2)-N(1)-C(6)	121.4 (7)	120.5 (6)	120.0 (7)
N(1)-C(2)-N(3)	117.8 (6)	118.4 (6)	119.8 (7)
C(2)-N(3)-C(4)	121.1 (6)	121.1 (6)	118.8 (7)
N(3)-C(4)-C(5)	120.3 (7)	119.9 (6)	122.6 (7)
C(4)-C(5)-C(6)	118.2 (8)	118.5 (7)	117.4 (8)
C(5)-C(6)-N(1)	121.2 (8)	121.5 (7)	121.3 (8)
C(1)-N(1)-C(6)	120.0 (7)	121.8 (6)	119.4 (7)
C(1)-N(1)-C(2)	118.5 (7)	117.6 (6)	120.5 (7)
N(1)-C(2)-O(2)	120.3 (7)	120.0 (6)	118.9 (7)
N(3)-C(2)-O(2)	121.9 (7)	121.6 (6)	121.3 (8)
N(3)-C(4)-N(4)	119.1 (7)	119.6 (6)	117.7 (7)
N(4)-C(4)-C(5)	120.6 (7)	120.5 (7)	119.7 (7)
Pt-N(3)-C(2)	116.0 (5)	117.5 (4)	
Pt-N(3)-C(4)	122.7 (5)	120.8 (5)	

Results and Discussion

Description of the Molecular Geometry of the *cis*-$[(NH_3)_2Pt(1\text{-}MeC)_2]^{2+}$ Cation and the Associated 1-MeC Base. The molecular geometry of the *cis*-$[(NH_3)_2Pt(1\text{-}MeC)_2]^{2+}$ cation and its interaction with the 1-MeC base of crystallization are depicted in the stereoview of Figure 2. In addition, two projection views

(40) Crystallographic programs employed include Wehe, Busing, and Levy's ORABS, Zalkin's FORDAP, Busing, Martin, and Levy's ORFLS (modified), Pippy and Ahmed's MEAN PLANE, and Johnson's ORTEP.

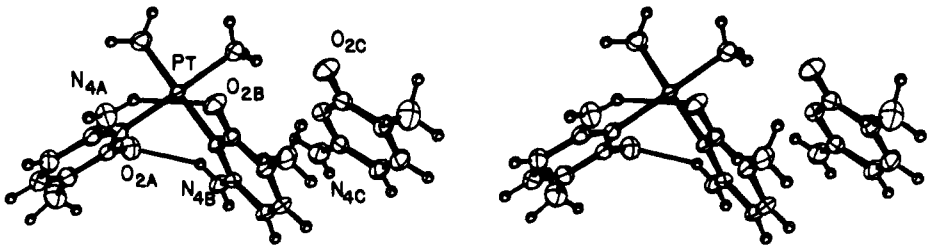

Figure 2. A stereoview of the *cis*-$[(NH_3)_2Pt(1\text{-MeC})_2]^{2+}$ cation and the associated 1-MeC base of crystallization. The intramolecular base···base hydrogen bonds are indicated by thin lines.

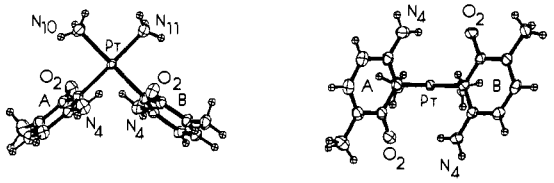

Figure 3. Two projection views of the *cis*-$[(NH_3)_2Pt(1\text{-MeC})_2]^{2+}$ cation: left, a view normal to the PtN_4 coordination plane; right, a view along the approximate twofold molecular axis.

of the complex cation are presented in Figure 3. One view is perpendicular to the PtN_4 coordination plane and the other is along the pseudo twofold axis of the complex ion. Bond lengths and angles in the primary coordination sphere and the 1-MeC bases are presented in Table III. The coordination geometry about the Pt(II) center is approximately square planar (Table IV). The four equatorial coordination sites are occupied by the N(3) heteroatoms of the two cis-bound 1-MeC bases (labeled A and B) and the N atoms of two ammonia molecules [$N(10)H_3$ and $N(11)H_3$]. The two coordinated 1-MeC ligands are arranged in a head-to-tail fashion such that the cation possesses approximate $2(C_2)$ molecular symmetry, Figure 3. The 1-MeC base of crystallization (labeled C) stacks in a head-to-head manner with one of the coordinated 1-MeC bases (B); see Figure 2. The mean interplanar separation between these stacked bases is 3.5 Å and the interbase dihedral angle is 11.4°.

The nearly equivalent Pt–N(3A) and Pt–N(3B) bond lengths of 2.031 (6) and 2.040 (6) Å are similar to those reported for the *cis*-$[(NH_3)_2Pt(1\text{-MeC})(9\text{-ethylguanine})]^{2+}$ cation,[26] 2.02 (1) Å, the *cis*-$[(NH_3)_2Pt(1\text{-MeC})(Thy = thymine anion)]^{+}$ cation,[41] 2.02 (2) Å, *trans*-dichloro(dimethyl sulfoxide)(cytidine)platinum(II),[42] 2.03 (1) Å, *trans*-dichloro(diisopropyl sulfoxide)(1-MeC)platinum(II),[43] 2.058 (7) Å, and the dimeric $[(en)Pt(5'\text{-CMP})]_2$ complex,[44] 2.06 Å. Within this series of compounds, there seems to be little systematic indication of a significant trans influence.[45] However, we do note for the accurately determined structures that the longest Pt–N(3) bond is for the S-bonded diisopropyl sulfoxide complex[43] and represents an extension of about 0.02 Å relative to the values presented here. The remaining bond lengths and angles within the primary coordination sphere are typical of those found in other Pt(II) complexes,[5] although the N(3A)–Pt–N(3B) angle at 92.6 (2)° is slightly larger than normally encountered [for example, the N(7)–Pt–N(3) angle is 90.6 (4)° in the *cis*-$[(NH_3)_2Pt(1\text{-MeC})(9\text{-ethylguanine})]^{2+}$ cation].[26]

It is probable that secondary interactions also play a role in the molecular conformation of the complex cation. The Pt···O(2A) and Pt···O(2B) distances of 3.020 (7) and 3.072 (7) Å are in agreement with the metal···O(2) distances observed in other Pt(II) and Pd(II) complexes with cytosine derivatives,[6a] 3.01–3.06 Å, and are consistent with the Pt···O(6) distances reported for several Pt(II)–N(1) bound 6-oxopurine complexes, 3.07–3.14 Å.[17] In all of these complexes the Pt atom is contiguous to the exocyclic oxygen atom, and the relatively long Pt···O distances may indicate some interaction with the metal center. These exocyclic oxo groups also form interligand, intracomplex hydrogen bonds to the exocyclic amino groups of alternate 1-MeC ligands [N(4B)···O(2A) = 3.03 Å, N(4A)···O(2B) = 3.10 (1) Å, see Figure 2 and Table V]. This represents the first time such interactions have been examined where the hydrogen atoms have been located from the diffraction data with any degree of certainty, although such interbase hydrogen bonding has been suggested earlier.[27] Additionally, an "intracomplex" hydrogen bond probably exists between one of the coordinated ammine ligands and the stacked 1-MeC base [N(11)···N(3C) = 3.07 (1) Å].

The six-atom framework of each of the three independent 1-MeC bases is approximately planar (Table IV), although we note that the uncoordinated base C is both the most planar and shows the least deviation of its exocyclic substituents from its plane of best fit. The deviations of the exocyclic functional groups from the planes of the coordinated ligands A and B can be taken as a first indication of intracomplex steric effects.

Table IV. Least-Squares Planes and the Deviation (in Å) of Individual Atoms from These Planes for *cis*-$[(NH_3)_2Pt(1\text{-MeC})_2](NO_3)_2 \cdot 1\text{-MeC}$

(a) Primary Coordination Sphere

$(-0.1133X + 0.0014Y - 0.9936Z = -1.8928$ Å)

Pt	−0.021 (0.3)	N(3B)	−0.013 (6)
N(3A)	0.024 (6)	N(10)	−0.014 (7)
		N(11)	0.024 (7)

(b) 1-Methylcytosine, Base A

$(0.5310X + 0.8084Y - 0.2542Z = 2.2130$ Å)

N(1A)	0.010 (7)	C(6A)	0.002 (7)
N(3A)	0.001 (6)	Pt*	−0.142 (0.3)
C(2A)	−0.011 (7)	N(3B)*	1.848 (6)
C(4A)	0.010 (7)	N(4A)*	0.041 (6)
C(5A)	−0.011 (8)	O(2A)*	−0.034 (6)
		C(1A)*	−0.001 (10)

(c) 1-Methylcytosine, Base B

$(0.9413X - 0.3199Y + 0.1079Z = 0.3966$ Å)

N(1B)	−0.012 (7)	C(6B)	−0.010 (7)
N(3B)	−0.012 (6)	Pt*	−0.322 (0.3)
C(2B)	0.023 (7)	N(3A)*	1.612 (6)
C(4B)	−0.010 (7)	N(4B)*	−0.070 (6)
C(5B)	0.021 (7)	O(2B)*	0.097 (6)
		C(1B)*	−0.120 (8)

(d) 1-Methylcytosine, Base C

$(-0.9874X + 0.1265Y - 0.0949Z = 1.5819$ Å)

N(1C)	0.002 (7)	C(6C)	−0.088 (9)
N(3C)	−0.009 (7)	N(4C)*	−0.015 (7)
C(2C)	0.006 (8)	O(2C)*	−0.017 (7)
C(4C)	0.003 (8)	C(1C)*	0.007 (11)
C(5C)	0.006 (8)		

[a] In each of the equations of the planes, X, Y, and Z are coordinates referred to the orthogonal axes X along the a axis, Y in the ab plane, and Z along the c^* axis. Atoms designated by an asterisk were given zero weight in calculating the planes; the atoms used to define the planes were given equal weight.

(41) Lippert, B.; Pfab, R.; Neugebauer, D. *Inorg. Chim. Acta* **1979**, *37*, L495.
(42) Melanson, R.; Rochon, F. C. *Inorg. Chem.* **1978**, *17*, 679.
(43) Lock, C. J. L.; Speranzini, R. A.; Powell, J. *Can. J. Chem.* **1976**, *54*, 53.
(44) Loule, S.; Bau, R. *J. Am. Chem. Soc.* **1977**, *99*, 3874.
(45) Appleton, T. G.; Clark, H. C.; Manzer, L. E. *Coord. Chem. Rev.* **1973**, *10*, 335.

Table V. Distances and Angles in the Interactions of the Type D-H···A for *cis*-$[(NH_3)_2Pt(1\text{-}MeC)_2](NO_3)_2\cdot 1\text{-}MeC$

D	H	D-H, Å	A[a]	H···A, Å	D···A, Å	∠D-H···A, deg
N(10)	H(101)	0.93	O(53)(a)	2.00	2.91 (1)	169
N(10)	H(103)	0.88	O(53)(b)	2.24	3.08 (1)	159
N(11)	H(111)	0.84	N(3C)	2.44	3.07 (1)	132[b]
N(4A)	H(4A1)	0.87	O(43)(c)	2.12	2.95 (1)	158
N(4A)	H(4A2)	0.88	O(2B)	2.34	3.10 (1)	145[b]
N(4B)	H(4B1)	0.87	O(2B)(d)	2.01	2.85 (1)	163
N(4B)	H(4B2)	0.89	O(2A)	2.25	3.01 (1)	147[b]
N(4C)	H(4C1)	0.87	O(2C)(d)	2.05	2.89 (1)	162
N(4C)	H(4C2)	0.88	O(51)(e)	2.10	2.91 (1)	154

[a] (a) $x, -1+y, z$; (b) $-x, 1-y, 1-z$; (c) $x, y, 1+z$; (d) $x, y, -1+z$; (e) $-x, 1-y, -z$. [b] Intracomplex hydrogen bonds.

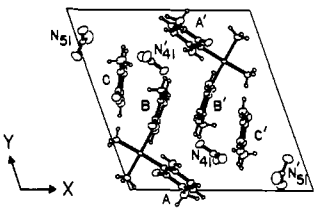

Figure 4. The (001) projection of the crystal structure of *cis*-$[(NH_3)_2Pt(1\text{-}MeC)_2](NO_3)_2\cdot 1\text{-}MeC$. Note the presence of extensive base/base and base/nitrate anion-stacking interactions, especially along the [110] crystallographic direction.

Finally, within the confines dictated by the eds's there are no significant differences in the bond lengths for the coordinated and uncoordinated 1-MeC bases (Table III). There are, however, some differences worthy of mention for the bond angles. We note that the C(2)–N(3)–C(4) bond angle increases while the N(1)–C(2)–N(3) and the N(3)–C(4)–C(5) bond angles decrease on complexation. Such a trend is consistent with the effect of binding other metal centers to N(3) of cytosine derivatives[6a] and the larger effects shown upon protonation or alkylation at N(3)[6a] relative to the molecular geometry of the free base 1-MeC.[46]

The Nitrate Anions and the Extended Crystal Structure. The range of observed N–O bond lengths (1.19–1.25 Å) and O–N–O bond angles (115–127°) are typical for systems in which the nitrate anions are not strongly coupled to other components in the structure.[47] The nitrate anions do, however, play a significant role in determining the overall crystalline motif, both through hydrogen bond formation and stacking interactions with the 1-MeC bases.

The most interesting aspect of the crystal packing is the rather extensive base/base and base/nitrate anion stacking shown in the (001) projection of Figure 4. The molecular overlap patterns for these interactions are depicted in Figure 5. The interaction of the coordinated base B and the uncoordinated base C (Figure 5A) has been commented on above. In addition, the B ligands of two complex cations self stack about centers of inversion of the type $(^1/_2,^1/_2,^1/_2)$ as shown in Figure 5B, with a mean separation between planes of 3.31 Å and a significant projection of the exocyclic methyl group of one base onto the ring of the other and vice versa. Each of the nitrate anions shows a similar overlay with a 1-MeC base [N(4) nitrate with the coordinated base A and nitrate N(5]) with the uncoordinated base C] as shown in Figure 4 and parts C and D of Figure 5.

Coupling of the layers parallel to the *ab* plane is achieved primarily through interbase hydrogen bonds of the type $N(4)\text{-}H_2\cdots O(2)$ (Table V and Figure 6). Only bases B and C are involved in these interactions between translationally related molecules [N(4B)···O(2B) = 2.85 (1) Å, N(4C)···O(2C) = 2.89 (1) Å]. On the basis of the N···O distances, these hydrogen bonding interactions are assumed to be considerably stronger than the intramolecular $N(4)H_2\cdots O(2)$ interaction described earlier. Other hydrogen-bonding interactions involving nitrate oxygen

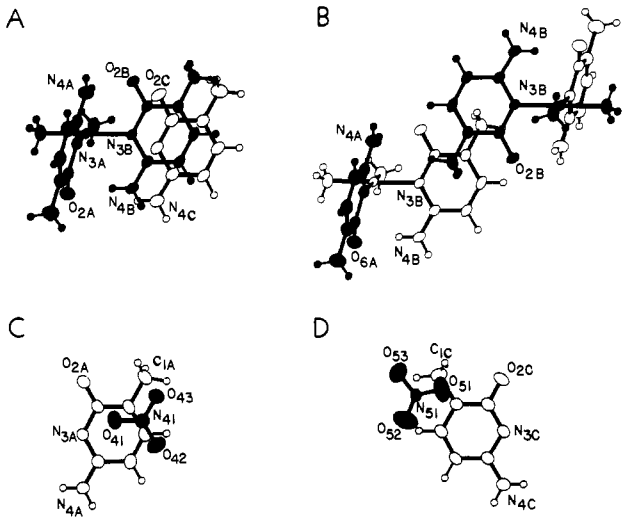

Figure 5. Details of the molecular overlaps in the structure of *cis*-$[(NH_3)_2Pt(1\text{-}MeC)_2](NO_3)_2\cdot 1\text{-}MeC$: (A) coordinated base(B)/base of crystallization (C) stacking (mean distance (D) = 3.5 Å; dihedral angle (DA) = 11.4°); (B) coordinated base(B)/coordinated base(B) stacking (D = 3.31 Å; DA = 0.0°); (C) nitrate anion(N(41))/coordinated base(A) stacking (D = 3.3 Å; DA = 9.6°); (D) nitrate anion(N(51))/base of crystallization (C) stacking (D = 3.1 Å; DA = 14.5°).

Table VI. Proton Chemical Shifts (δ) Downfield from Me_4Si in $Me_2SO\text{-}d_6$ for *cis*-$[(NH_3)_2Pt(1\text{-}MeC)_2](NO_3)_2\cdot 1MeC$

	H(5)	H(6)	-N(4)H$_2$ H	-N(4)H$_2$ H*
(a) coordinated 1-MeC bases (types A and B)[b]	5.92[a]	7.80[a]	8.61	8.82
(b) uncoordinated 1-MeC base (type C)	5.68[a]	7.62[a]	7.1 (br)	
(c) 1-MeC[c]	5.59	7.52	6.9	

[a] Doublets, $J_{H-H} \approx 7.2$ Hz. [b] The ammine proton resonance occurs as a broad triplet (δ 4.38 ($J_{Pt-H} \approx 26$ Hz)). [c] Values for 1-methylcytosine taken from: Marzilli, L. G.; Chang, C.-H.; Caradonna, J. P.; Kistenmacher, T. J. *Adv. Mol. Relaxation Interact. Proc.* 1979, *15*, 85. The small difference between the chemical shifts for (b) and (c) may be due to environmental effects.

atoms as acceptors and the exocyclic amino groups on bases A and C and both coordinated ammine ligands as donors are present in the structure (Table V and Figure 6).

^{1}H NMR Spectrum. We have been able to obtain the ^{1}H NMR spectrum of crystals of *cis*-$[(NH_3)_2Pt(1\text{-}MeC)_2](NO_3)_2\cdot 1\text{-}MeC$ dissolved in $Me_2SO\text{-}d_6$ (0.15 M). Relevant chemical shift data for the coordination compound are compared to those for the free base 1-MeC[48] in Table VI. As expected, resonances for the complexed 1-MeC bases (A and B) and the uncomplexed bases (C) are observed with an experimental ratio of their integrated intensities of 1.93 (8) (ideally, 2.0) consistent with the formulation

(46) Rossi, M.; Kistenmacher, T. J. *Acta Crystallogr., Sect. B* **1977**, *B33*, 3962.

(47) Szalda, D. J.; Kistenmacher, T. J.; Marzilli, L. G. *Inorg. Chem.* **1975**, *14*, 2623 and references therein.

(48) Marzilli, L. G.; Chang, C.-H.; Caradonna, J. P.; Kistenmacher, T. J. *Adv. Mol. Relaxation Interact. Processes* **1979**, *15*, 85.

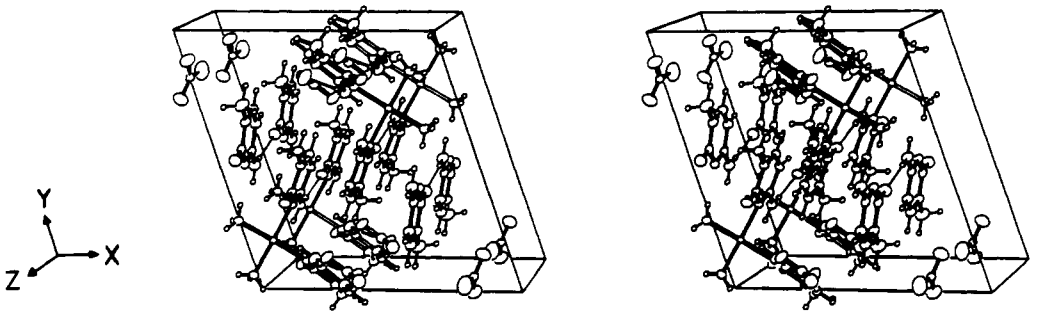

Figure 6. A stereoview of the crystal structure of *cis*-$[(NH_3)_2Pt(1\text{-}MeC)_2](NO_3)_2 \cdot 1\text{-}MeC$. Note in particular the base···base and nitrate···base intermolecular hydrogen bonds (denoted by thin lines) along the *c* axis.

based on the X-ray data and results.

Several interesting features emerge from the spectral data. First, the C–H resonances [H(5) and H(6), see Figure 1] of the coordinated 1-MeC ligands are shifted downfield by ~0.2 ppm (probably due to the Pt binding) from the same resonances for the uncoordinated base. Similar downfield shifts for H(5) and H(6) of coordinated cytosine derivatives have been reported by Kong and Theophanides[49,50] for $[(dien)Pt(Cyd)]^{2+}$ and [(dien)-Pt(5′-CMP)] and by Chu, Duncan, and Tobias[51] for $[(en)Pt(Cyd)(H_2O)]^{2+}$ and $[(en)Pt(Cyd)_2]^{2+}$. However, while ^{195}Pt coupling to the protons of the coordinated ammine ligands (J_{Pt-H} = 26 Hz) is readily observed, we, like Chu et al.,[51] do not observe ^{195}Pt–H(5) coupling as reported by Kong and Theophanides.[49] In this regard, various contributions (notably chemical shift anisotropy relaxation) to the diminishing of ^{195}Pt–^{1}H and ^{195}Pt–^{13}C coupling constants have recently been explored by Lallemand, Soulie, and Chottard.[52]

A second interesting observation is that while the NH_2 resonance of the uncoordinated 1-MeC base is a broad singlet (virtually unshifted from that of the free 1-MeC base, Table VI) as is typically found for amino resonances which normally undergo free rotation on the NMR time scale, *two* NH resonances are observed for the coordinated 1-MeC ligands. Both of these NH resonances are strongly shifted downfield (~1.5 ppm) relative to the uncoordinated base. The observation of two resonances is consistent with the intracomplex steric effects and hydrogen bonding observed in the solid-state structure, since in addition to the Pt binding at N(3) one of the amino protons is intramolecularly hydrogen bonded.[53]

Lastly, we recall that Chu, Duncan, and Tobias[51] found that the ^{13}C NMR resonances for C(6) of the cytosine base and C(2′), C(3′), and C(4′) of the sugar residue occurred as two signals (separated by 0.3–0.5 ppm) for the $[(en)Pt(Cyd)_2]^{2+}$ cation. These authors[51] suggested that the presence of two signals could be attributed to two isomers of the complex cation, one in which the Cyd ligands are arranged in a head-to-tail fashion (as found here for the bis(1-MeC) complex cation) and a second in which the Cyd ligands are arranged in a head-to-head manner. There is, however, an alternative explanation which can be invoked.

Following the arguments of Cramer and Dahlstrom,[54] we note that there are two diastereomers of the $[(en)Pt(Cyd)_2]^{2+}$ cation in which the cytosine bases are arranged in a head-to-tail fashion. In order to observe the separate ^{1}H NMR signals for each of the diastereomers of a bis(N(7)-bound guanosine)Pt complex cation, Cramer and Dahlstrom[54] found it necessary to employ the sterically bulky chelate *N,N,N′,N′*-tetramethylethylenediamine to inhibit interconversion of the diastereomers by rapid rotation about the Pt–N(7) bonds of the guanosine ligands. If, however, as suggested long ago for Ni(II)[55] and Pt(II)[56] complexes containing ortho-disubstituted pyridine ligands, the barrier to rotation about the Pt–N(3) bonds of the Cyd ligands (with the ortho substituents $-NH_2$ and $=O$) is large, then separate signals for the diastereomers of $[(en)Pt(Cyd)_2]^{2+}$ should be observable and could account for the results of Chu, Duncan, and Tobias.[51] We prefer this latter explanation for the ^{13}C spectral results for $[(en)Pt(Cyd)_2]^{2+}$ as we believe that the head-to-head isomer proposed by Chu et al.[51] would be sterically prohibited by unfavorable interligand interactions.

Table VII. Pyrimidine Ring Binding Sites in Various Nucleosides and the Nature of the Substituents Adjacent to the Site

nucleoside	pyrimidine ring-binding site	adjacent exocyclic substituents
adenosine (Ado)	N(1)	$-H, -N(6)H_2$
inosine (Ino)	N(1)[a]	$-H, =O(6)$
guanosine (Guo)	N(1)[a]	$-N(2)H_2, =O(6)$
cytidine (Cyd)	N(3)	$-N(4)H_2, =O(2)$
thymidine (Thd) uridine (Urd)	N(3)[a]	$=O(2), =O(4)$

[a] Requires proton release prior to or concomitant with metal binding.

Convention for Comparing the Conformational Features of *cis*-Bis(pyrimidine ring-bound)platinum(II) Complexes and Implications Thereof. In the previous section, we have described in detail the molecular and crystal structure of the coordination compound *cis*-$[(NH_3)_2Pt(1\text{-}MeC)_2](NO_3)_2 \cdot 1\text{-}MeC$. Over the past few years several other crystal structures for compounds of the type $[(amine)_2Pt(B)(B')]$, where the bases B and B′ are pyrimidine or purine derivatives, have been reported.[5,6] In the present context we are particularly interested in those systems which show coordination at an endocyclic N atom of a pyrimidine ring (Table VII) and the possible role that the exocyclic functional groups adjacent to these sites play in the determination of the molecular conformation. It became clear to us in the course of attempting to compare the conformational parameters in the present *cis*-$[(NH_3)_2Pt(1\text{-}MeC)_2]^{2+}$ cation to those exhibited by related systems that some convention for describing such parameters in a systematic way needed to be defined. We consider the most important geometrical parameters to be the interbase dihedral angle (B/B′), the base/PtN_4 coordination plane dihedral angles (B/PtN_4 and B′/PtN_4), and the perpendicular displacement of the Pt atom from the base to which it is attached (ΔPt from base B and ΔPt′ from base B′). A compendium of these parameters for the *cis*-$[(NH_3)_2Pt(1\text{-}MeC)_2]^{2+}$ cation and for three other *cis*-bis(pyrimidine ring-bound)Pt(II) complexes is given in Table VIII, and the B/B′ and B,B′/PtN_4 dihedral angles are illustrated in Figure 7.

In preparing Table VIII and Figure 7, we have adopted the following convention.

(a) Base/Base Dihedral Angle (B/B′). The base/base dihedral angle, as with all other dihedral angles, may be defined as an angle or its supplement. In order to achieve a meaningful comparison

(49) Kong, P. C.; Theophanides, T. *Inorg. Chem.* **1974**, *13*, 1167.
(50) Kong, P. C.; Theophanides, T. *Inorg. Chem.* **1974**, *13*, 1981.
(51) Chu, G. Y. H.; Duncan, R. E.; Tobias, R. S. *Inorg. Chem.* **1977**, *16*, 2625.
(52) Lallemand, J. Y.; Soulie, J.; Chottard, J. C. *J. Chem. Soc., Chem. Commun.* **1980**, 436.
(53) Sorrell, T.; Epps, L. A.; Kistenmacher, T. J.; Marzilli, L. G. *J. Am. Chem. Soc.* **1978**, *100*, 5756.
(54) Cramer, R. E.; Dahlstrom, P. L. *J. Am. Chem. Soc.* **1979**, *101*, 3679.
(55) Chatt, I.; Shaw, B. L. *J. Chem. Soc.* **1960**, 1718.
(56) Orchin, M.; Schmidt, P. J. *Inorg. Chim. Acta Rev.* **1968**, *2*, 123.

Table VIII. Relevant Conformational Parameters for *cis*-Bis(pyrimidine ring-bound)platinum(II) Complexes

complex	ref	dihedral angles, deg B/B′	dihedral angles, deg B/PtN$_4$	dihedral angles, deg B′/PtN$_4$	ΔPt, Å	ΔPt′, Å	∠N$_B$-Pt-N$_{B'}$, deg
[(NH$_3$)$_2$Pt(1-MeC)$_2$]$^{2+}$	this study	102	102 (1-MeC$_A$)	101 (1-MeC$_B$)	−0.14 (1-MeC$_A$)	−0.32 (1-MeC$_B$)	92.6 (2)
[(NH$_3$)$_2$Pt(3′-CMP)$_2$]$^{2-}$ [d]	*a*	94	112		−0.17		94 (1)
[(NH$_3$)$_2$Pt(1-MeC)(Thy)]$^+$	*b*	86	108 (Thy)	114 (1-MeC)	−0.13 (Thy)	+0.02 (1-MeC)	89 (1)
[(en)Pt(7,9-Dmhyp)$_2$]$^{2+}$ [d]	*c*	64	126		+0.32		92.8 (2)

[a] Wu, S.; Bau, R. *Biochem. Biophys. Res. Commun.* 1979, *88*, 1435. [b] Lippert, B.; Ffab, R.; Neugebauer, D. *Inorg. Chim. Acta* 1979, *37*, 1495. [c] Kistenmacher, T. J.; de Castro, B.; Wilkowski, K.; Marzilli, L. G. *J. Inorg. Biochem.*, in press. [d] Molecular twofold symmetry present.

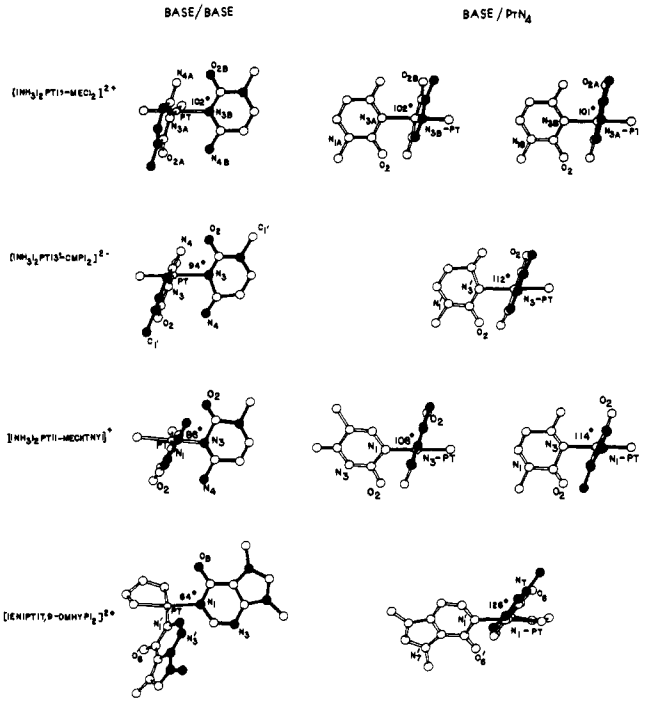

Figure 7. Illustrations and magnitudes for the base/base and base/PtN$_4$ dihedral angles in four *cis*-bis(pyrimidine ring-bound)Pt(II) complexes. Abbreviations used are as follows: 1-MeC = 1-methylcytosine; 3′-CMP = cytidine 3′-monophosphate; THY = monoanion of thymine; 7,9-DMHYP = 7,9-dimethylhypoxanthine; en = ethylenediamine. For primary references see the text.

among different compounds, it is advantageous to view each molecule or molecular ion in a standard orientation from which a visual distinction can ordinarily be made between angles greater than or less than 90°. This can be achieved by confining one of the two bases to the plane of the paper and to the right of the second base, which projects outward toward the viewer (see column 1 of Figure 7). Such a convention yields a B/B′ interbase dihedral angle of 102° for the present cation; in view of the restrictive interbase interactions, it is clear to us that the definition of the interbase dihedral as 102° is superior to that of its supplement 78°. Similarly, we quote the average B/B′ dihedral angle for the *cis*-[(NH$_3$)$_2$Pt(3′-CMP)$_2$]$^{2-}$ anion as 96° in contrast to the earlier report of the supplementary angle 84°.[27]

(b) Base/PtN$_4$ Coordination Plane Dihedral Angles (B/PtN$_4$ and B′/PtN$_4$). To view and compare the B/PtN$_4$ dihedral angle, we oriented the molecule such that the N$_B$′–Pt bond, where N$_B$ is the coordinated atom of the base associated with the dihedral angle B/PtN$_4$, is perpendicular to the plane of the paper with N$_B$ nearest the viewer. The N$_B$′–Pt bond is then positioned horizontally and to the left of the diagram. A similar procedure is followed to illustrate the B′/PtN$_4$ dihedral angle. The dihedral angles quoted are those indicated by column 2 of Figure 7. For molecules possessing twofold symmetry, there is, of course, only one unique B/PtN$_4$ dihedral angle. The utility of this convention is illustrated for the complex cation *cis*-[(NH$_3$)$_2$Pt(1-MeC)(Thy)]$^+$ where the B/PtN$_4$ dihedral angles were originally reported[41] as 114° for the thymine anion and 72° for the 1-MeC base; at first glance such a description might indicate a need for explaining a difference of some 42° in B/PtN$_4$ dihedral angles. Whereas in the present description, Table VIII and Figure 7, there is only a 6° difference indicated which can be easily rationalized.

(c) Perpendicular Displacement of the Pt Atom from the Base to Which It Is Attached (ΔPt and ΔPt′). The sense (+ or −) of the perpendicular displacement of the Pt atom from the plane of the base to which it is attached is determined as follows.

(i) +: the displacement of the Pt atom out of the plane of the first base is in the same direction as the displacement of the coordinated N atom of the second base.

(ii) −: the displacement of the Pt atom out of the plane of the first base is in the opposite direction to the displacement of the coordinated N atom of the second base.

An examination of the conformational parameters as given in Table VIII and pictorially represented in Figure 7 reveals the following trends. As the number of exocyclic functional groups contiguous to the Pt atom binding site increases from (1 + 1) for the [(en)Pt(7,9-Dmhyp)$_2$]$^{2+}$ cation[17] to (2 + 1) for the *cis*-[(NH$_3$)$_2$Pt(1-MeC)(Thy)]$^+$ cation[41] to (2 + 2) for the *cis*-[(NH$_3$)$_2$Pt(1-MeC)$_2$]$^{2+}$ cation, (1) the interbase dihedral angle B/B′ increases smoothly, (2) the B/PtN$_4$ and B′/PtN$_4$ dihedral angles progressively assume smaller values, and (3) the sense of the (ΔPt, ΔPt′) displacements changes from (+,+) to (+,−) to (−,−) so as to further minimize unfavorable interligand interactions. These trends suggest that as the number of exocyclic substituents ortho to the Pt binding sites increases, intracomplex steric factors become more determinative of the molecular conformation. We expect this deduction to be generally applicable to square-planar complexes with cis-coordinated ortho-substituted ligands.

The culmination of the above trends in the sterically crowded *cis*-[(NH$_3$)$_2$Pt(1-MeC)$_2$]$^{2+}$ cation is, we believe, particularly noteworthy. It is our contention that the conformational parameters in this complex cation are primarily dictated by *intracomplex* steric effects and that the observed dihedral angles and Pt atom displacements represent the best compromise in terms of minimizing the ligand/ligand and ligand/PtN$_4$ steric interactions. The dominance of intracomplex steric interactions in *cis*-bis(N(3)-bound)Pt complexes of cytosine is expected to carry over directly to *cis*-bis(N(1)-bound)Pt complexes of guanine as the nature and number of functional groups adjacent to the Pt binding sites (Table VII) are exactly the same.[17] In contrast, for *cis*-bis(N(7)-bound)Pt(II) complexes of purine derivatives (which in a formal sense have no substituents other than –H adjacent to the metal binding site),[5] the B/B′ and B,B′/PtN$_4$ dihedral angles are expected to be determined by competition between intracomplex and intercomplex interactions. When favorable intracomplex base–base interactions dominate, as in [(tn)Pt(Me-5′-GMP)$_2$]^0, the B/B′ dihedral angle is as small as 40°.[25] However, in other instances, where either intercomplex base stacking occurs or counterions are present, the B/B′ dihedral angle may be large and dictated by intercomplex effects. For example, for the cations [(en)Pt-(Guo)$_2$]$^{2+}$ and *cis*-[(NH$_3$)$_2$Pt(Guo)$_2$]$^{2+}$ where there is considerable intermolecular base stacking, the B/B′ dihedral angle is ~70°.[18,19] The effect of the counterion on the B/B′ dihedral angle is apparent when the molecular structures of the NO_3^- and PF_6^- salts of the [(en)Pt(1,3,9-trimethylxanthine)$_2$]$^{2+}$ cation are compared.[57] Their

(57) Orbell, J. D.; de Castro, B.; Wilkowski, K.; Marzilli, L. G.; Kistenmacher, T. J., to be submitted for publication.

respective B/B′ dihedral angles are 71 and 87°, a significant difference which can apparently be attributed only to the presence in the structure of the different anions.[57]

In regard to the perturbation of a DNA structure upon binding of the *cis*-$(NH_3)_2Pt^{II}$ moiety in an intrastrand cross-linking mode for regions of high Guo-Cyd content,[5-6,8,15-16] the above deductions are suggestive of varying degrees of stereochemical interference with the native motif of the DNA duplex. As noted in the Introduction, various modes of intrastrand cross-linking may be envisioned. All of these demand, of course, some degree of local denaturation or premelting in order to accommodate the formation of the cross-link. The degree of local denaturation of the duplex to accommodate a G[N(7)]-Pt-G[N(7)] mode may, however, be slight in comparison to that demanded by a linkage of the type C[N(3)]-Pt-C[N(3)], although the occurrence of the latter may be rare as its formation is mitigated against by strong interbase repulsion. Finally, if one accepts the notion[58] that cancer cells are deficient in their ability to excise defects from strands of DNA, then such cells may find defects imposed by cross-links of the type C[N(3)]-Pt-C[N(3)] particularly difficult to repair.[59]

Acknowledgment. This investigation was supported by the National Institutes of Health, Public Health Service Grants GM 20544 and GM 29222. We thank Matthey Bishop, Inc. for a loan of K_2PtCl_4.

Supplementary Material Available: Tables of nonhydrogen atom anisotropic thermal parameters and of parameters for the hydrogen atoms and a list of calculated and observed structure factor amplitudes (46 pages). Ordering information is given on any current masthead page.

(58) Rosenberg, B. *Biochimie* **1978**, *60*, 859.

(59) While this paper was in the submission stage, the structures of three other Pt(II)-N(3)bound 1-methylcytosine complexes have been reported: (a) Lippert, B.; Lock, C. J. L.; Speranzini, R. A. *Inorg. Chem.* **1981**, *20*, 335. (b) Lippert, B.; Lock, C. J. L.; Speranzini, R. A. *Ibid.* **1981**, *20*, 808.

Ferric Ion-Specific Sequestering Agents. 7. Synthesis, Iron-Exchange Kinetics, and Stability Constants of N-Substituted, Sulfonated Catechoylamide Analogues of Enterobactin[1]

Vincent L. Pecoraro, Frederick L. Weitl,[2] and Kenneth N. Raymond*[3]

Contribution from the Department of Chemistry and Materials and Molecular Research Division, Lawrence Berkeley Laboratory, University of California, Berkeley, California 94720.
Received October 30, 1980

Abstract: Two analogues of enterobactin are reported which exhibit (i) stability to base-catalyzed hydrolysis of the central ring, (ii) water solubility, and (iii) N-substitution to block peptidase hydrolysis of the amide bonds. The first compound 1,3,5-tris(*N*-methyl-*N*-(2,3-dihydroxysulfobenzoyl)aminomethyl)benzene (Me_3MECAMS) was prepared, via the amide of trimesoyl chloride and $MeNH_2$, in four steps and 6% overall yield. The proton-dependent formation constant ($\log K^* = \log([FeL^{6-}][H^+]^3)/([Fe^{3+}][H_3L^{6-}])$) is 5.21, which gives an equilibrium concentration of $[Fe^{3+}]$ at pH 7.4 of 1×10^{-27} M for 10^{-5} M Me_3MECAMS and 10^{-6} M total Fe^{3+}. The estimated formation constant ($\log \beta_{110}$) is 41. At low pH the FeL^{6-} complex undergoes a series of one-proton reactions which probably gives a tris-"salicylate" complex formed by the carbonyl and ortho-catechol oxygens of the 2,3-dihydroxybenzoyl units. After 6 h, in the presence of 6 mM ascorbate ($T = 37$ °C, $\mu = 0.05$ M), Me_3MECAMS (6.0 mM) removed 3.7% of the ferric ion initially sequestered by the iron-storage protein ferritin. The human iron-transport protein transferrin releases iron to Me_3MECAMS with a pseudo-first-order rate constant of 1.9×10^{-3} min^{-1} (ligand concentration 2×10^{-4} M, $T = 25$ °C, $\mu = 0.10$ M). This rate is comparable to that of enterobactin and other catechoyl amide sequestering agents and greatly exceeds that of desferrioxamine B (Desferal), the current drug of choice in treating iron overload. Two related compounds have been prepared in which the catechol ring is attached to the amide nitrogen through a methylene group, with amide formation with an acetyl group. In 1,3,5-tris(*N*-acetyl-*N*-(2,3-dihydroxysulfobenzyl)aminomethyl)benzene [NAcMECAMS] and its unsulfonated precursor, the amide linkage of the catechoyl amides such as Me_3MECAMS has been shifted from an endo position relative to the benzene and catechol rings to an exo position in which the amide carbonyl is not conjugated with the catechol ring and cannot form a stable chelate ring in conjunction with a catechol oxygen. In comparison with Me_3MECAMS, the protonation of NAcMECAMS proceeds by an initial two-proton step in contrast to the one-proton reactions typical of the catechoyl amides, which can form a "salicylate" mode of coordination involving the amide carbonyl group. Also as a result of the removal of the carbonyl group from conjugation with the catechol ring, the acidity of NAcMECAMS is less than Me_3MECAMS. While the estimated $\log \beta_{110} = 40$ is approximately the same as for Me_3MECAMS, the effective formation constant ($\log K^*$) and pM ($-\log [Fe_{aq}^{3+}]$) values are lower (4.0 and 25.0, respectively).

It is established that virtually all organisms need iron.[4] Human beings maintain a total inventory of ca. 5 g in the adult through a complex process of iron transport and storage.[5] In this light, it is a well documented fact that, in excess, Fe^{3+} is very toxic. Indeed, acute iron overload (primarily from ingestion of iron supplement preparations by infants) is one of the most common

(1) Previous paper in this series: Harris, W. R.; Raymond, K. N.; Weitl, F. L., *J. Am. Chem. Soc.* **1981**, *103*, 2667-75.

(2) Materials and Molecular Research Division, Lawrence Berkeley Laboratory, Berkeley, CA 94720.

(3) To whom correspondence should be addressed at the Department of Chemistry, University of California, Berkeley, CA 94720.

(4) Neilands, J. B., Ed. "Microbial Iron Transport: A Comprehensive Treatise"; Academic Press: New York, 1974.

(5) Lewis, A. E. "Principles of Hematology"; Meridith Corporation: New York, 1970.

0002-7863/81/1503-5133$01.25/0